

## Dynamic characterization of 3D printed mechanical metamaterials with tunable elastic properties

Naghavi Zadeh, Mohammad; Alijani, Farbod; Chen, Xianfeng; Dayyani, Iman; Yasaei, Mehdi; Mirzaali, Mohammad J.; Zadpoor, Amir A.

**DOI**

[10.1063/5.0047617](https://doi.org/10.1063/5.0047617)

**Publication date**

2021

**Document Version**

Final published version

**Published in**

Applied Physics Letters

**Citation (APA)**

Naghavi Zadeh, M., Alijani, F., Chen, X., Dayyani, I., Yasaei, M., Mirzaali, M. J., & Zadpoor, A. A. (2021). Dynamic characterization of 3D printed mechanical metamaterials with tunable elastic properties. *Applied Physics Letters*, 118(21), Article 211901. <https://doi.org/10.1063/5.0047617>

**Important note**

To cite this publication, please use the final published version (if applicable). Please check the document version above.

**Copyright**

Other than for strictly personal use, it is not permitted to download, forward or distribute the text or part of it, without the consent of the author(s) and/or copyright holder(s), unless the work is under an open content license such as Creative Commons.

**Takedown policy**

Please contact us and provide details if you believe this document breaches copyrights. We will remove access to the work immediately and investigate your claim.

# Dynamic characterization of 3D printed mechanical metamaterials with tunable elastic properties

Cite as: Appl. Phys. Lett. **118**, 211901 (2021); <https://doi.org/10.1063/5.0047617>

Submitted: 15 February 2021 . Accepted: 04 May 2021 . Published Online: 24 May 2021

 Mohammad Naghavi Zadeh,  Farbod Alijani,  Xianfeng Chen, Iman Dayyani, Mehdi Yasaee,  Mohammad J. Mirzaali, and  Amir A. Zadpoor



View Online



Export Citation



CrossMark

## ARTICLES YOU MAY BE INTERESTED IN

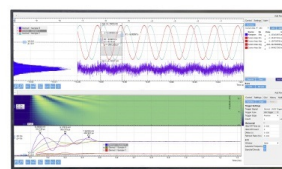
[3D gradient auxetic soft mechanical metamaterials fabricated by additive manufacturing](#)  
Applied Physics Letters **118**, 141904 (2021); <https://doi.org/10.1063/5.0043286>

[Enhanced light-matter interactions at photonic magic-angle topological transitions](#)  
Applied Physics Letters **118**, 211101 (2021); <https://doi.org/10.1063/5.0052580>

[Myths and truths about optical phase change materials: A perspective](#)  
Applied Physics Letters **118**, 210501 (2021); <https://doi.org/10.1063/5.0054114>

## Challenge us.

What are your needs for  
periodic signal detection?



Zurich  
Instruments

# Dynamic characterization of 3D printed mechanical metamaterials with tunable elastic properties

Cite as: Appl. Phys. Lett. **118**, 211901 (2021); doi: [10.1063/5.0047617](https://doi.org/10.1063/5.0047617)

Submitted: 15 February 2021 · Accepted: 4 May 2021 ·

Published Online: 24 May 2021



View Online



Export Citation



CrossMark

Mohammad Naghavi Zadeh,<sup>1,a)</sup>  Farbod Alijani,<sup>2</sup>  Xianfeng Chen,<sup>2</sup>  Iman Dayyani,<sup>1</sup> Mehdi Yasaei,<sup>1</sup> Mohammad J. Mirzaali,<sup>3,a)</sup>  and Amir A. Zadpoor<sup>3</sup> 

## AFFILIATIONS

<sup>1</sup>School of Aerospace, Transport, and Manufacturing, Cranfield University, Bedford MK43 0AL, United Kingdom

<sup>2</sup>Department of Precision of Microsystems Engineering, Delft University of Technology (TU Delft), Mekelweg 2, 2628 CD Delft, The Netherlands

<sup>3</sup>Department of Biomechanical Engineering, Delft University of Technology (TU Delft), Mekelweg 2, 2628 CD Delft, The Netherlands

<sup>a)</sup>Authors to whom correspondence should be addressed: [mo.zadeh.aero@gmail.com](mailto:mo.zadeh.aero@gmail.com) and [m.j.mirzaali@tudelft.nl](mailto:m.j.mirzaali@tudelft.nl)

## ABSTRACT

Mechanical metamaterials are advanced engineering materials that exhibit unusual properties that cannot be found in nature. The elastic properties (i.e., elastic modulus and Poisson's ratio) of mechanical metamaterials can be tuned by changing the geometry of their fundamental unit cells. This allows for the design of metamaterial lattices with targeted quasi-static properties. However, it is not clear how these freedoms contribute to the dynamic properties of mechanical metamaterials. We, therefore, used experimental modal analysis, numerical simulations, and analytical models to study the dynamic response of meta-structures with different values of the Poisson's ratio. We show that Poisson's ratio strongly affects the damping properties of the considered mechanical metamaterials. In particular, we found an inverse relationship between the damping ratio and the absolute value of the Poisson's ratio of the meta-structures. Our results suggest that architected meta-structures similar to those studied could be tailor-made to improve the dissipative performance of mechanical systems. Geometrical design could play an important role in this regard by providing the possibility to tune the various types of quasi-static and dynamic properties of such mechanical metamaterials.

Published under an exclusive license by AIP Publishing. <https://doi.org/10.1063/5.0047617>

Mechanical metamaterials belong to the class of designer materials whose unprecedented tailor-made properties originate from their designs at a smaller scale.<sup>1</sup> One of these unconventional properties is the possibility to tune the Poisson's ratio through the design of their micro-architecture. In particular, the materials with negative (the so-called auxetics<sup>2</sup>) and zero values of the Poisson's ratio (ZPR)<sup>3,4</sup> are often studied due to their unique properties and functionalities that are interesting for a wide range of potential applications. In addition to the meta-structures with one single value of the Poisson's ratio, the Poisson's ratio of a meta-structure can be adjusted locally<sup>5</sup> or globally to achieve novel functionalities, such as shape-shifting or shape-morphing.<sup>6</sup>

The micro-architectures of mechanical metamaterials are often made of one or more unit cells that are repeated in three dimensions to create a (semi-)regular lattice structure. By adjusting the geometry and spatial arrangement of the fundamental unit cells, one can achieve

specific values of the Poisson's ratio. The hexagonal (with positive or negative angle)<sup>2</sup> and chiral unit cells<sup>7</sup> are some examples of the unit cell geometries used in the past for the design of mechanical metamaterials with tunable values of the Poisson's ratio. This suggests that only by the design of the unit cell's geometry one can reach a broad range of elastic properties<sup>8,9</sup> or even extend this range through random integration of unit cells in the design space of the lattice structures,<sup>10–12</sup> which allows for targeting very specific combinations of mechanical properties and/or advanced functionalities.

ZPR and auxetic structures have several applications in the aeronautical<sup>4,13</sup> and biomedical industries.<sup>14–16</sup> These classes of the mechanical metamaterials have been successfully designed and tested under quasi-static conditions; however, it is still unclear how these unconventional properties can influence the dynamic response of ZPR and auxetic structures. Additionally, it is important to understand how the freedom in devising the geometry of unit cells can aid in obtaining

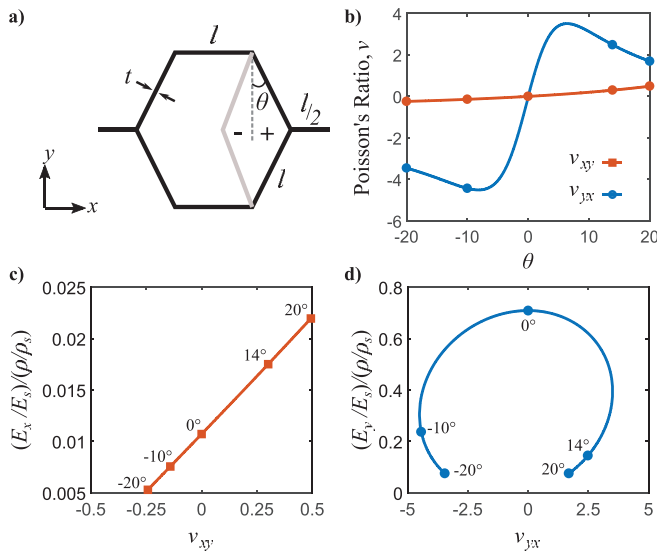


**FIG. 1.** (a) Unit cell design of the hexagonal geometry used for designing the specimens where the angle  $\theta$  can possess different values while other parameters are constant. (b) Variations of the Poisson's ratio in two planar directions are plotted as a function of the angle  $\theta$ , which shows that larger Poisson's ratios are achieved for two samples. The variation of the non-dimensional equivalent elastic modulus as a function of the corresponding Poisson's ratio is plotted in (c) the  $x$ - and (d)  $y$ -directions.

metamaterials with tunable modal properties. Therefore, understanding the evolution of the dynamic characteristics (e.g., damping properties, natural frequencies, and mode shapes) of mechanical metamaterials and the capabilities to tune those dynamic properties independently is of high importance.

Here, we used a combination of analytical solutions, numerical modeling, and experimental modal analysis (EMA) to investigate the effect of the Poisson's ratio on the dynamic response of additively manufactured (AM) metamaterials with hexagonal lattice geometries. Moreover, we studied the effects of the angle of the ligaments and Poisson's ratio on the dynamic characteristics of the metamaterials, namely natural frequencies, mode shapes, and damping ratios.

AM specimens with five different designs were fabricated from commercial polylactic acid (PLA) filaments and using a fused deposition modeling (FDM) 3D printer (Ultimaker 2+, The Netherlands). The elastic modulus,  $E_s$ , and Poisson's ratio,  $\nu_s$ , of the PLA filaments were, respectively, 3500 MPa and 0.36 while the density of the material,  $\rho_s$ , was 1250 kg/m<sup>3</sup>. In our designs, the unit cells had a ligament thickness of  $t = 0.6$  mm and a length of  $l = 5$  mm [Fig. 1(a)]. Moreover, the out-of-plane thickness of all the specimens was  $h = 5$  mm. While the length of the ligaments remained constant, the values of the Poisson's ratio in two directions were tuned by changing the angle  $\theta$  in each unit cell [Fig. 1(b)]. A range of negative, zero, and positive values of the Poisson's ratio was achieved using five designs with  $\theta$  angles of  $-20^\circ$ ,  $-10^\circ$ ,  $0^\circ$ ,  $14^\circ$ , and  $20^\circ$ . The relative density of the structure ( $\rho$ ), elastic modulus, and Poisson's ratio of the resulting cellular materials were calculated using the method proposed by Malek and Gibson<sup>9</sup> (see the [supplementary material](#), Part A). The effective values of the Poisson's ratio and elastic modulus of the lattice structures in the  $x$  and  $y$ -directions [Figs. 1(b)–1(d)] were within the ranges of the values predicted by the cellular material theory.<sup>17</sup>

In Figs. 2(a)–2(c), we show some examples of the 3D printed specimens with a negative ( $\theta = -20$ ), zero ( $\theta = 0$ ), and positive ( $\theta = 20$ ) value of the Poisson's ratio.

We used experimental modal analysis (EMA) to measure the natural frequencies and damping ratio, as well as to visualize the mode shapes of the manufactured metamaterial lattice structures. The test setup (Fig. 3) included a signal generator (OFV-5000, Polytec) that controlled the excitation through an electrodynamic shaker (Type 4809, Bruel&Kaer) and a laser Doppler vibrometer (LDV) (PSV-400, Polytec) was used for probing the motion. In order to obtain a higher quality signal from LDV, reflective tapes (3M 340) were attached on the surface of the test specimens and the measurements were performed over a large number of points so that the mode shapes could be properly captured. To excite the specimens, a periodic chirp function over 200 Hz frequency band was applied and the natural frequencies and damping ratios were extracted using the Polytec software PSV 8.5 that uses the circle fit method to estimate the modal parameters.

The boundary conditions considered in this work are all-edge free, which can be best obtained in a full-floating state.<sup>18,19</sup> In our experiments, however, we suspended the lattice structures vertically

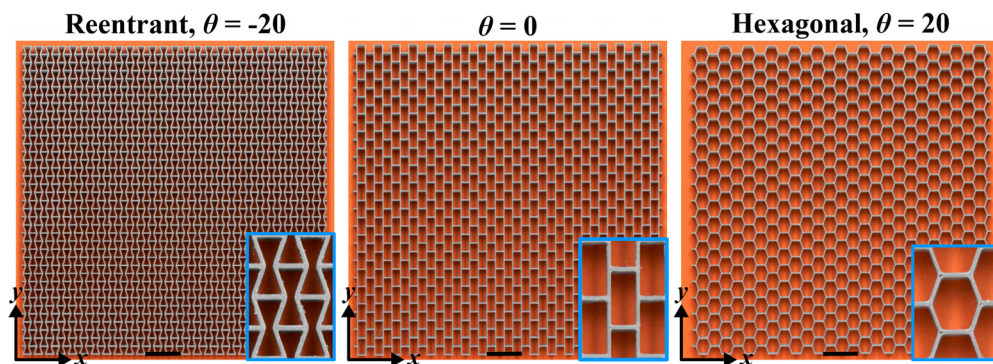


**FIG. 2.** Specimens were additively manufactured using an Ultimaker FDM 3D printer and PLA filaments. Three designs with negative, zero, and positive values of the Poisson's ratio are shown where the design of the unit cell is illustrated in a magnified view. The thickness of each ligament is  $t = 0.6$  mm and the scale bar represents 20 mm.

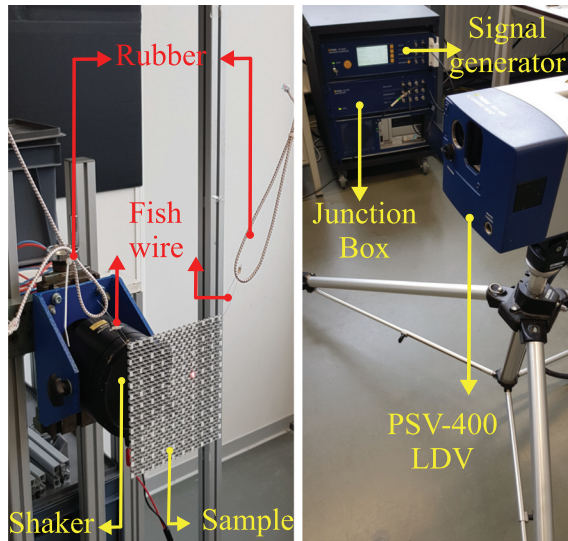


**FIG. 3.** Modal test setups consisting of a shaker, the test specimen, a Polytec LDV sensor, and a signal generator. Rubber bands and fishing wires were used to suspend the sample, and a shaker was used to excite the specimen through a stinger.

using rubber bands and fishing wires attached to their top corner and tuned the tension of the bands in such a way that the elastic modes of the structure were well-separated from its rigid body modes. This setup has shown to replicate with very good accuracy the all-edge free boundary conditions.<sup>20,21</sup> After suspending the structures, a shaker was connected to the specimens using a stinger with an offset (20–30 mm) from its center.

We modeled our samples as moderately thick plates with equivalent homogenous properties obtained by methodology from Malek and Gibson<sup>9</sup> (see the [supplementary material](#), Part A). The method for deriving the equations of motion and studying the vibrations of all-edge free rectangular plates has been explained by Alijani and Amabili<sup>18,22</sup> (see the [supplementary material](#), Part B), which is employed here to study the natural mode shapes.

The FE analysis of the full-scale samples was conducted by Abaqus (ver 2018, Simulia, Providence, USA) using solid elements with an approximate global size of 0.3 mm (see the [supplementary material](#), Part C). The Lanczos solver was used to solve the eigenvalue problem numerically and the results were obtained for the 0–200 Hz frequency band. Six rigid body modes were obtained due to the free boundary conditions of the specimens.

The natural frequencies ( $\Omega$ ) of the first five resonance modes of each sample are presented in [Fig. 4](#) including the experimental and numerical values. The experimental natural frequencies follow the values from numerical simulations where relative errors between two methods are due to the manufacturing and test setup imperfections. The trends of the results were, however, consistent between the experiments and simulations, with the resonance frequencies increasing with the ligament angle. It should be noted that density of the samples decreases with increasing the angle from negative to positive values that results in increasing the natural frequencies as expected. Therefore, the higher the metamaterial density is the larger mode count in a certain frequency band is expected, which has an inverse correlation with the angle  $\theta$ .

The mode shapes of the lattice structures were either symmetric (S) or anti-symmetric (A) with respect to the axis of symmetry of the plates. Similar mode shapes have been previously reported for all-edge free composite sandwich structures with positive Poisson's ratio (PPR)<sup>22</sup> [[Fig. 5\(a\)](#)]. With the change of the ligament angle and, thus, effective elastic properties, the mode shapes of the meta-structures changed ([Fig. 5](#)). This change was particularly apparent in the SS and SA modes because symmetric deformations are more sensitive to the value of the effective elastic modulus along the two planar directions. For those modes, the Poisson's ratio modified the value and sign of the coupling between the elastic modulus in the  $x$ - and  $y$ -directions that resulted in anticlastic, uniaxial, or synclastic curvatures.

For a zero value of the Poisson's ratio [[Fig. 5\(b\)](#)], we observed uniaxial deformations, whereas synclastic curvature in SS and SA mode shapes was observed for the negative values of the Poisson's ratio [[Fig. 5\(c\)](#)]. The third mode shape in all the three categories of meta-structures was symmetric around the  $y$ -axis. However, the Poisson's ratio  $\nu_{xy}$  was about one-tenth of  $\nu_{yx}$ . The synclastic and anti-clastic curvatures in this mode were, therefore, small. There was also a good agreement between the analytical, computational, and experimental mode shapes.

Comparing the damping ratios,  $\zeta$ , of the first three modes obtained from EMA for the different designs of the meta-structures showed the damping coefficient of the SS mode is maximum for zero and the positive values of the Poisson's ratio, while it is minimum for the specimens with the negative values of the Poisson's ratio [[Fig. 6\(a\)](#)]. The average damping ratios of the zero-angle (i.e., zero Poisson's ratio) structure for the first three modes were 0.026, 0.043, and 0.034, respectively. These values are higher than the corresponding values for the meta-structures with  $\theta = 14^\circ$  and  $\theta = -10^\circ$  [[Fig. 6\(a\)](#)].

Studying the variation of the damping ratio vs angle  $\theta$  suggested that the damping ratio has a local extremum for each natural mode at zero angle for the specimens with  $-20^\circ < \theta < 20^\circ$ . For the first mode,  $\zeta$  reduced for  $\theta = 14^\circ$  and  $\theta = -10^\circ$  but started increasing when the absolute value of the angle reached  $20^\circ$  [[Fig. 6\(a\)](#)]. A similar trend was also observed for the second and third mode shapes [[Fig. 6\(a\)](#)]. The observed behavior suggested that the absolute value of the Poisson's ratio was inversely related to the damping ratio. The minimum damping ratio, therefore, occurred for angles close to the extremum of the absolute value of the Poisson's ratio [[Fig. 6\(a\)](#)]. The fact that in metamaterials with hexagonal geometry damping can be tuned using the angle  $\theta$  is a potentially important finding. However, the correlation discussed for the damping ratio must be further validated using another technique to ensure the independence of the result from the test method. For this reason, we aimed at obtaining the loss factor of the fabricated meta-structures using a quasi-static analysis.

The loss factor,  $\eta = \Psi/2\pi = \Delta U_p/(2\pi U_p)$ , is described as the energy loss per radian of a vibratory system.<sup>23</sup> We used this parameter as the second verification parameter to establish the relationship between damping and the angle  $\theta$  of our meta-structures. Here, parameter  $\Psi$  is the specific damping capacity (SDC) that is a measure for the global damping of the structure,<sup>24,25</sup>  $\Delta U_p$  is the dissipated energy in a hysteresis cycle, and  $U_p$  is the total strain energy. In order to measure the loss factor, quasi-static tests were conducted using an Instron tensile test machine and a loading rate of 1 mm/min up to 1% strain in the  $y$ -direction [[Fig. 6\(b\)](#)]. Loading in the  $y$ -direction is

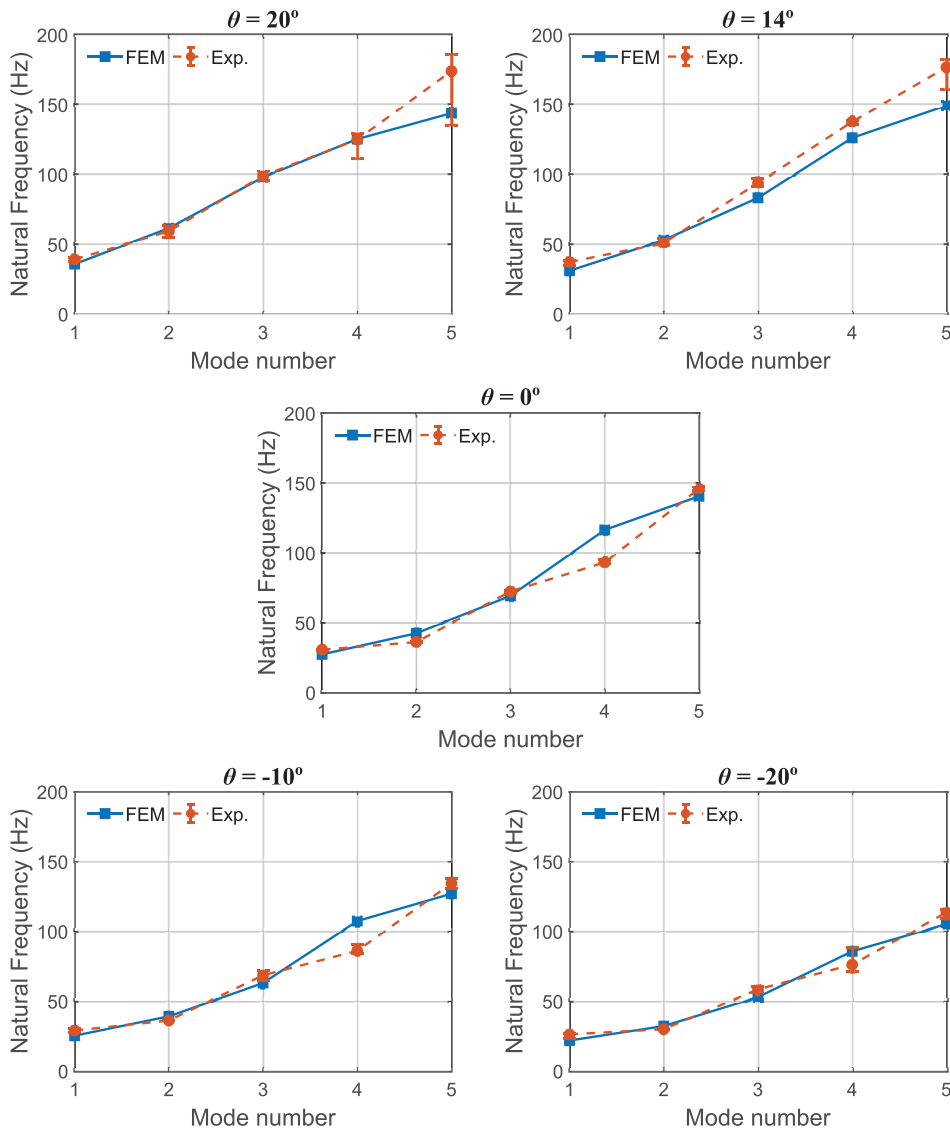


FIG. 4. Natural frequencies of the five metamaterial specimens obtained using experimental modal analysis and FE simulations for the first five modes.

considered because the effective modulus  $E_y$  is an order of magnitude larger than  $E_x$  and has a larger contribution to the stiffness of the structure. The hysteresis curves of the specimens were obtained for five cycles and specific damping capacity,  $\Psi$ , was plotted vs the angle  $\theta$  and cycle number [Fig. 6(c)]. The SDC for the first cycle was much larger than the next ones because the main irreversible fracture event in the structure happened during the first loading cycle.<sup>26</sup> After the second cycle, the slope of the SDC curve became smooth and maintained approximately a constant value.

In Table I, the loss factor values are presented for all types of meta-structures. These values show a trend of variation with angle  $\theta$  that is comparable to the one presented by the damping ratios obtained using modal analysis. The loss factor and damping coefficient had a maximum value for the zero-degree design. When the angle  $\theta$  was reduced or increased, the loss factor and damping coefficient first decreased and then increased [Figs. 6(a) and 6(c)]. There was,

therefore, an inverse relationship between the loss factor of the hexagonal structures and the absolute value of the Poisson's ratio  $\nu_{yx}$ .

In order to evaluate the damping merit of the different designs, a figure of merit is used<sup>23,26</sup> that is proportional to the ratio of the cubic root of the elastic modulus to the density of the structure,  $E^{1/3}/\rho$ . In this paper, the damping merit index (DMI) is obtained using the relationship  $\left(\frac{E_y}{E_x}\right)^{1/3} \times \Psi / \left(\frac{\rho}{\rho_s}\right)$  [Fig. 6(d)], where  $E_y$  is the equivalent modulus in the  $y$ -direction, while  $E_x$  and  $\rho_s$  are, respectively, the elastic modulus and density of the constituting material. Since DMI is correlated with the ratio of the effective modulus to the density, its trend vs Poisson's ratio is similar to Fig. 1(d). Our results showed that the DMI of the meta-structures considered here are strongly dependent on the dominant effective modulus (i.e.,  $E_y$ ). Therefore, if the damping merit of the cellular structure is of relevance for any specific application, the meta-structures with a zero value of the Poisson's ratio provide better

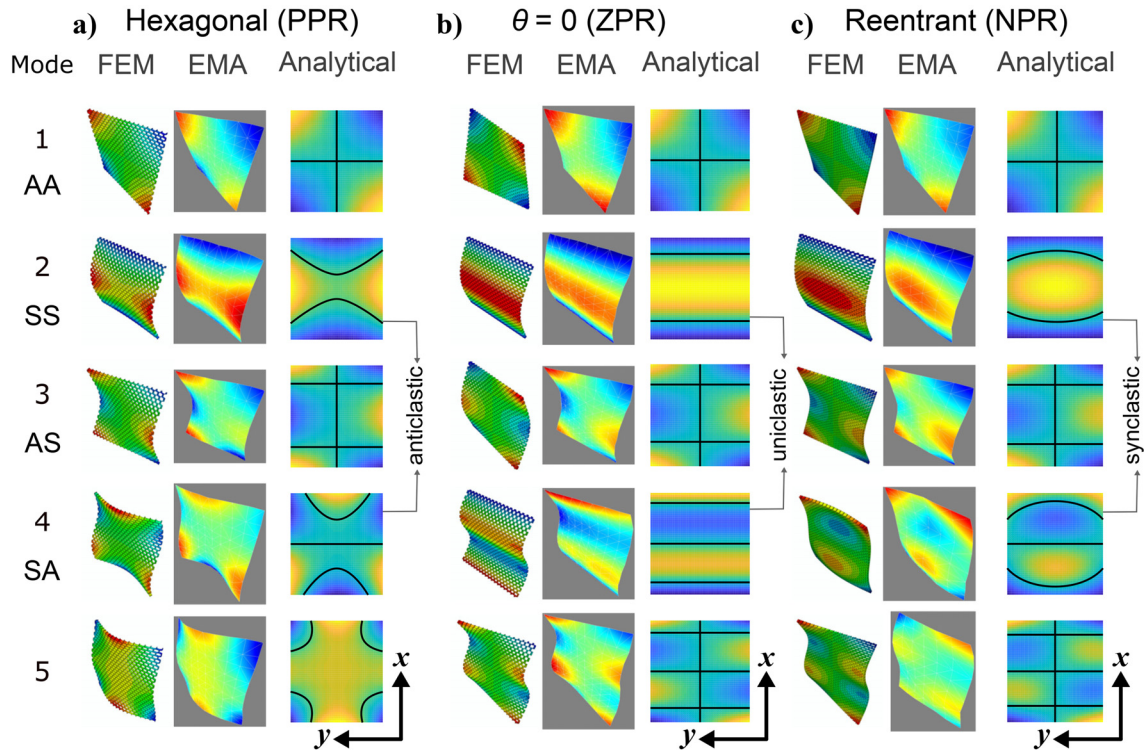


**FIG. 5.** The first five mode shapes of the specimens with (a) positive Poisson's ratio (PPR), (b) zero Poisson's ratio (ZPR), and (c) negative Poisson's ratio (NPR). The term "re-entrant" refers to hexagonal geometry with  $\theta < 0$  that result in negative values of the Poisson's ratio. The black lines in the analytical plots represent the approximate zero-displacement paths of each mode shape. The effects of the Poisson's ratio on the curvature coupling of the symmetrically deformed shapes are highlighted. In the mode shape nomination, the first and second letter stand for the symmetry (S) or asymmetry (A) of the deformation with respect to the central axis along the x- and y-direction, respectively.

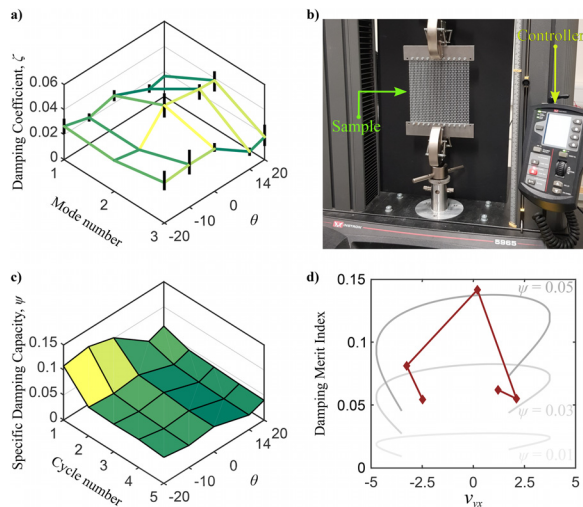


**FIG. 6.** (a) Average damping coefficients of the first three natural modes of the test specimens obtained from EMA where the black lines represent the error bars of each mode. (b) The tensile test setup used for the cyclic quasi-static analysis of the metamaterials hysteresis. (c) Variation of the loss factor in each cycle for the five design of meta-structures. (d) DMI of the test specimens (red line) as a function of the Poisson's ratio and the geometric locus of the constant loss factor DMI curves for three different loss factors.

performance than the meta-structures with a negative or positive value of the Poisson's ratio.

Tuning the dynamic properties of lattice meta-structures have potential applications in light-weight load-bearing structures with enhanced energy harvesting properties.<sup>27</sup> In addition, the dynamic response of metamaterials is of relevance to shock-absorbent devices<sup>28</sup> widely used in sports equipment, biomedical, automotive, and aeronautical industries. The dynamically controlled metamaterials can also be equipped with other forms of excitations, such as electromagnetic, temperature, or light to exhibit multi-functional properties.<sup>29,30</sup> Finally, such adjustable dynamic properties can provide additional freedom for the design of adaptive metamaterials, such as soft-actuators<sup>31</sup> or tunable (compliant) mechanisms<sup>32,33</sup> at different length-scales.

**TABLE I.** Loss factor values from the fifth hysteresis cycle for the hexagonal structures.

$\theta^\circ$	$\eta = \Psi/2\pi$
-20	0.0165
-10	0.0140
0	0.0159
14	0.0092
20	0.0124

As a conclusion of this paper, we studied the dynamic response of 3D printed mechanical metamaterials with tunable elastic properties. The metamaterial had a hexagonal lattice structure whose ligation angle could be used for obtaining materials with different effective values of the elastic modulus and Poisson's ratio. The dynamic response of the meta-structures was studied using experimental modal analysis, an analytical model, and computational models. We studied the damping performance of these hexagonal metamaterials and found that the geometrical designs considered here could be used for the development of metamaterials with tunable damping ratios. The meta-structures with a zero value of the Poisson's ratio exhibited a local extremum value of the damping coefficient when compared to those with the angles of  $\theta = -10^\circ$  and  $\theta = 14^\circ$ . The damping performance decreased as the absolute value of the Poisson's ratio increased. This trend was also verified by the hysteresis curves obtained using tensile cyclic quasi-static tests where the specific damping capacity was determined as a measure of structural dissipation. The meta-structures studied here have many potential applications in (adaptable) mechanical systems across different length scales where the dynamic response in general and the damping characteristics in particular can be tuned through the geometrical design of the underlying lattice structures.

See the [supplementary material](#) for details of the analytical method and numerical simulations.

#### DATA AVAILABILITY

The data that support the findings of this study are available from the corresponding author upon reasonable request.

#### REFERENCES

- <sup>1</sup>A. A. Zadpoor, "Mechanical meta-materials," *Mater. Horiz.* **3**, 371–381 (2016).
- <sup>2</sup>H. M. A. Kolkun and A. A. Zadpoor, "Auxetic mechanical metamaterials," *RSC Adv.* **7**, 5111–5129 (2017).
- <sup>3</sup>M. N. Zadeh, I. Dayyani, and M. Yasaei, "Fish Cells, a new zero Poisson's ratio metamaterial—Part II: Elastic properties," *J. Intell. Mater. Syst. Struct.* **31**, 2196–2210 (2020).
- <sup>4</sup>M. Naghavi Zadeh, I. Dayyani, and M. Yasaei, "Fish Cells, a new zero Poisson's ratio metamaterial—Part I: Design and experiment," *J. Intell. Mater. Syst. Struct.* **31**(13), 1617–1637 (2020).
- <sup>5</sup>R. Hedayati, M. J. Mirzaali, L. Vergani, and A. A. Zadpoor, "Action-at-a-distance metamaterials: Distributed local actuation through far-field global forces," *APL Mater.* **6**, 36101 (2018).
- <sup>6</sup>M. J. Mirzaali, S. Janbaz, M. Strano, L. Vergani, and A. A. Zadpoor, "Shape-matching soft mechanical metamaterials," *Sci. Rep.* **8**, 1–7 (2018).
- <sup>7</sup>W. Wu, W. Hu, G. Qian, H. Liao, X. Xu, and F. Berto, "Mechanical design and multifunctional applications of chiral mechanical metamaterials: A review," *Mater. Des.* **180**, 107950 (2019).
- <sup>8</sup>L. J. Gibson and M. F. Ashby, *Cellular Solids: Structure and Properties* (Cambridge University Press, 1999).
- <sup>9</sup>S. Malek and L. Gibson, "Effective elastic properties of periodic hexagonal honeycombs," *Mech. Mater.* **91**, 226–240 (2015).
- <sup>10</sup>M. J. Mirzaali, A. Caracciolo, H. Pahlavani, S. Janbaz, L. Vergani, and A. A. Zadpoor, "Multi-material 3D printed mechanical metamaterials: Rational design of elastic properties through spatial distribution of hard and soft phases," *Appl. Phys. Lett.* **113**, 241903 (2018).
- <sup>11</sup>M. J. Mirzaali, H. Pahlavani, and A. A. Zadpoor, "Auxeticity and stiffness of random networks: Lessons for the rational design of 3D printed mechanical metamaterials," *Appl. Phys. Lett.* **115**, 021901 (2019).
- <sup>12</sup>M. J. Mirzaali, R. Hedayati, P. Vena, L. Vergani, M. Strano, and A. A. Zadpoor, "Rational design of soft mechanical metamaterials: Independent tailoring of elastic properties with randomness," *Appl. Phys. Lett.* **111**, 051903 (2017).
- <sup>13</sup>K. R. Olympio and F. Gandhi, "Zero Poisson's ratio cellular honeycombs for flex skins undergoing one-dimensional morphing," *J. Intell. Mater. Syst. Struct.* **21**, 1737–1753 (2010).
- <sup>14</sup>G. R. Douglas, A. S. Phani, and J. Gagnon, "Analyses and design of expansion mechanisms of balloon expandable vascular stents," *J. Biomech.* **47**, 1438–1446 (2014).
- <sup>15</sup>G. C. Engelmayr, M. Cheng, C. J. Bettinger, J. T. Borenstein, R. Langer, and L. E. Freed, "Accordion-like honeycombs for tissue engineering of cardiac anisotropy," *Nat. Mater.* **7**, 1003–1010 (2008).
- <sup>16</sup>P. Soman, D. Y. Fozdar, J. W. Lee, A. Phadke, S. Varghese, and S. Chen, "A three-dimensional polymer scaffolding material exhibiting a zero Poisson's ratio," *Soft Matter* **8**, 4946 (2012).
- <sup>17</sup>F. Scarpa and G. Tomlinson, "Theoretical characteristics of the vibration of sandwich plates with in-plane negative Poisson's ratio values," *J. Sound Vib.* **230**, 45–67 (2000).
- <sup>18</sup>F. Alijani and M. Amabili, "Theory and experiments for nonlinear vibrations of imperfect rectangular plates with free edges," *J. Sound Vib.* **332**, 3564–3588 (2013).
- <sup>19</sup>X. Chen, A. Keskeker, F. Alijani, and P. G. Steeneken, "Rigid body dynamics of diamagnetically levitating graphite resonators," [arXiv:2006.01733](https://arxiv.org/abs/2006.01733) (2020).
- <sup>20</sup>F. Alijani, M. Amabili, G. Ferrari, and V. D. Alessandro, "Nonlinear vibrations of laminated and sandwich rectangular plates with free edges. Part 2: Experiments & comparisons," *Compos. Struct.* **105**, 437–445 (2013).
- <sup>21</sup>K. Sinha, N. K. Singh, M. M. Abdalla, R. De Breucker, and F. Alijani, "A momentum subspace method for the model-order reduction in nonlinear structural dynamics: Theory and experiments," *Int. J. Non-Linear Mech.* **119**, 103314 (2020).
- <sup>22</sup>F. Alijani and M. Amabili, "Nonlinear vibrations of laminated and sandwich rectangular plates with free edges. Part 1: Theory and numerical simulations," *Compos. Struct.* **105**, 422–436 (2013).
- <sup>23</sup>M. F. Ashby, T. Evans, N. A. Fleck, J. W. Hutchinson, H. N. G. Wadley, and L. J. Gibson, *Metal Foams: A Design Guide* (Elsevier, 2000).
- <sup>24</sup>C. W. Bert, "Material damping: An introductory review of mathematic measures and experimental technique," *J. Sound Vib.* **29**, 129–153 (1973).
- <sup>25</sup>M. Carfagni, E. Lenzi, and M. Pierini, "The loss factor as a measure of mechanical damping," *Proc. SPIE* **3243**, 580–584 (1998).
- <sup>26</sup>L. Salari-Sharif, T. A. Schaedler, and L. Valdevit, "Energy dissipation mechanisms in hollow metallic microlattices," *J. Mater. Res.* **29**, 1755–1770 (2014).
- <sup>27</sup>Z. Chen, B. Guo, Y. Yang, and C. Cheng, "Metamaterials-based enhanced energy harvesting: A review," *Phys. B: Condens. Matter* **438**, 1–8 (2014).
- <sup>28</sup>C. Yang, M. Boorugu, A. Dopp, J. Ren, R. Martin, D. Han, W. Choi, and H. Lee, "4D printing reconfigurable, deployable and mechanically tunable metamaterials," *Mater. Horiz.* **6**, 1244–1250 (2019).
- <sup>29</sup>K. Fan and W. J. Padilla, "Dynamic electromagnetic metamaterials," *Mater. Today* **18**, 39–50 (2015).
- <sup>30</sup>L. Liu, L. Kang, T. S. Mayer, and D. H. Werner, "Hybrid metamaterials for electrically triggered multifunctional control," *Nat. Commun.* **7**, 1–8 (2016).
- <sup>31</sup>L. M. Nash, D. Kleckner, A. Read, V. Vitelli, A. M. Turner, and W. T. M. Irvine, "Topological mechanics of gyroscopic metamaterials," *Proc. Natl. Acad. Sci.* **112**, 14495–14500 (2015).
- <sup>32</sup>L. Ma, L. He, and Y. Ni, "Tunable hierarchical wrinkling: From models to applications," *J. Appl. Phys.* **127**, 111101 (2020).
- <sup>33</sup>L. Meng, J. Shi, C. Yang, T. Gao, Y. Hou, L. Song, D. Gu, J. Zhu, P. Breitkopf, and W. Zhang, "An emerging class of hyperbolic lattice exhibiting tunable elastic properties and impact absorption through chiral twisting," *Extreme Mech. Lett.* **40**, 100869 (2020).